

# Effects of fracture connectivity on Rayleigh wave dispersion

Gabriel E. Quiroga<sup>1</sup>, J. Germán Rubino<sup>2</sup>, Santiago G. Solazzi<sup>1</sup>, Nicolás D. Barbosa<sup>3</sup>, and Klaus Holliger<sup>1</sup>.

<sup>1</sup>Applied and Environmental Geophysics Group, Institute of Earth Sciences, University of Lausanne, Lausanne, Switzerland.

<sup>2</sup>CONICET, Centro Atómico Bariloche-CNEA, San Carlos de Bariloche, Argentina.

<sup>3</sup>Department of Earth Sciences, University of Geneva, Geneva, Switzerland.



# Summary

In this work, we consider changes in the degree of fracture network connectivity to explore the effects that this parameter has on Rayleigh wave velocity dispersion.

We apply a numerical upscaling method in a Monte-Carlo-type manner to determine the effective body wave velocities for two end-member-type scenarios of fracture connectivity.

A reservoir model is then generated based on the results of the upscaling procedure, for which we evaluate the Rayleigh wave phase and group velocities.

The results indicate that Rayleigh wave velocity dispersion is sensitive to the degree of fracture connectivity and, thus, could, for example, be used to infer the evolution of this parameter in the context of passive seismic monitoring.

# Introduction

The characterization of fractured rock formations is of increasing importance for a wide range of applications such as hydrocarbon exploration, CO<sub>2</sub> storage and geothermal applications.

In that context, passive seismic monitoring has proven to be a reliable and non-intrusive method of following the evolution of geothermal reservoirs (Taira et. al. 2018; Obermann et. al. 2015).

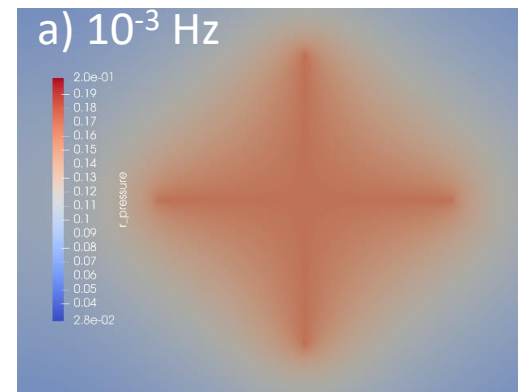
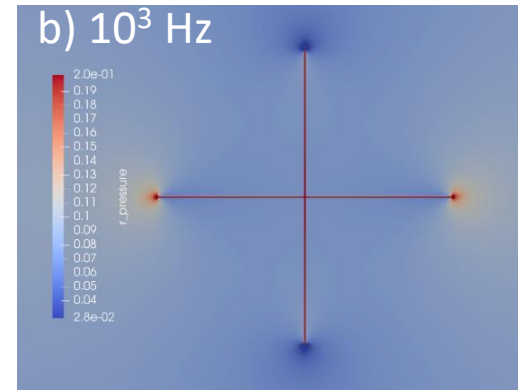
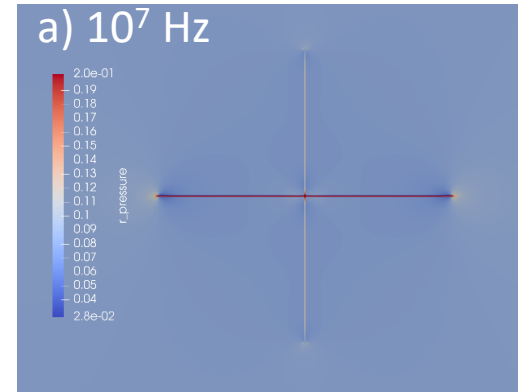
This monitoring is mostly based on the inversion of Rayleigh wave velocity dispersion, but the analysis often neglects wave-induced fluid pressure diffusion (FPD) effects, which can have a significant impact on the seismic response of fractured rocks (Rubino et. al. 2013, 2014, 2017).

# Introduction

Two manifestations of FPD arise in fractured rocks: Fracture-to-background FPD (FB-FPD) and fracture-to-fracture FPD (FF-FPD) (Rubino et. al. 2013, 2014). FB-FPD dominates the response at lower frequencies and FF-FPD at higher frequencies.

We aim to explore the impact of fracture-related FPD effects on Rayleigh wave velocity dispersion. To this end, we consider two end-member-type cases of connectivity on a crystalline rock. We compute their effective body wave velocity employing a poroelastic upscaling procedure in a Monte-Carlo-type manner. The effective velocities are then incorporated in a reservoir model and we evaluate the sensitivity of Rayleigh wave velocity dispersion to fracture network connectivity.

© AUTHORS. ALL RIGHTS RESERVED



A time-harmonic vertical displacement is applied to the upper boundary of a sample containing two intersecting fractures, the resulting pressure is mapped at different frequencies.

In a) we see the results for a high frequency of  $10^7$  Hz, showing that the pressure is confined to the horizontal fracture (Elastic equivalent case). In b) we see the results for a frequency of  $10^3$  Hz, where we can observe that the pressure is homogeneous between the connected fractures (FF-FPD). In c) for a frequency of  $10^{-3}$  Hz, we can observe how there is pressure exchange between the fractures and the background rock (FB-FPD).

# Methodological Background

In order to obtain the P- and S-wave velocities of fractured rock samples, taking into account FPD effects, we use a poroelastic upscaling approach based on the one presented in Rubino et. al. (2016).

This upscaling procedure is implemented as a finite-element code called “Parrot”, which is able to perform the procedure for complex fracture networks (Hunziker et. al. 2018; Favino et. al. 2020).

We aim to obtain the seismic response of two cases of connectivity on fractured granite samples: one with a fracture network composed of completely isolated fractures, and another where all fractures have at least a connection with another fracture.

# Methodological Background

Computational constraints impede the characterization of samples large enough to guarantee representativeness of the response of the connected or unconnected stochastic fracture networks.

We follow a Monte Carlo approach to characterize the formation (Rubino et. al. 2009), generating a large number of realizations of the upscaling procedure and considering the mean of the P- and S-wave velocities obtained to be the effective velocities of the samples.

The convergence of the Monte Carlo approach is determined by the stabilization of the standard deviation of the corresponding body wave velocity as the number of realizations grows.

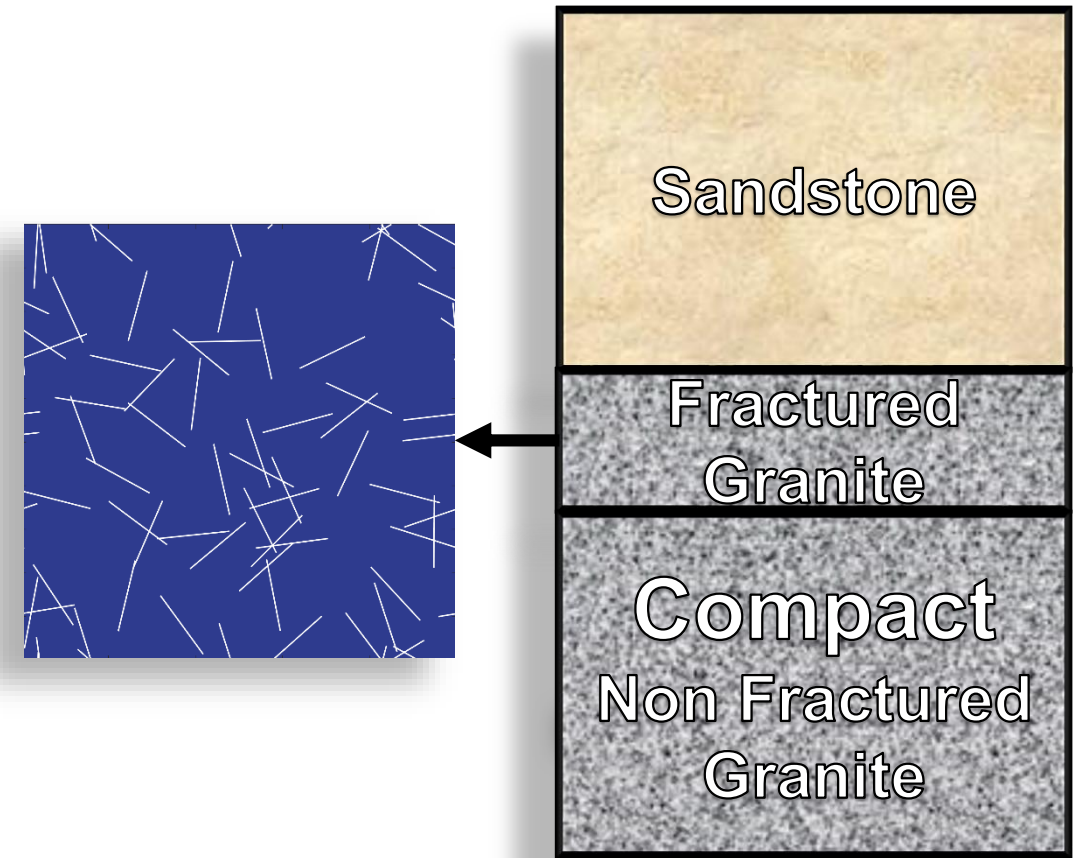
The samples employed contain fractures with constant length and aperture and a homogenous distribution of orientations and random fracture positions, for these reasons, the velocities obtained by this procedure are isotropic.

# Methodological Background

To compute the Rayleigh wave velocity dispersion curves associated with the reservoir models, we populate a model of velocity and density with depth using the previously inferred effective velocities.

Rayleigh wave phase and group velocities are obtained by using a root searching algorithm to obtain the zeroes of the Rayleigh determinant,  $D(k, w)$ , where  $k$  is the wavenumber and  $w$  is the angular frequency.

To compute the Rayleigh determinant, we use the Fast Delta Matrix method presented by Buchen and Ben Hador (1996) and the root searching algorithm employed is the secant method.



Schematic illustration of the considered three-layer model. The panel on the left shows a representative sample associated with the fractured reservoir model analyzed in this work.



# Effective body wave velocities

The synthetic rock samples used for the poroelastic upscaling procedures are squares with a side length of 50 cm containing fractures with length and aperture of 12 cm and 0.4 mm respectively. The fracture density is 0.5%.

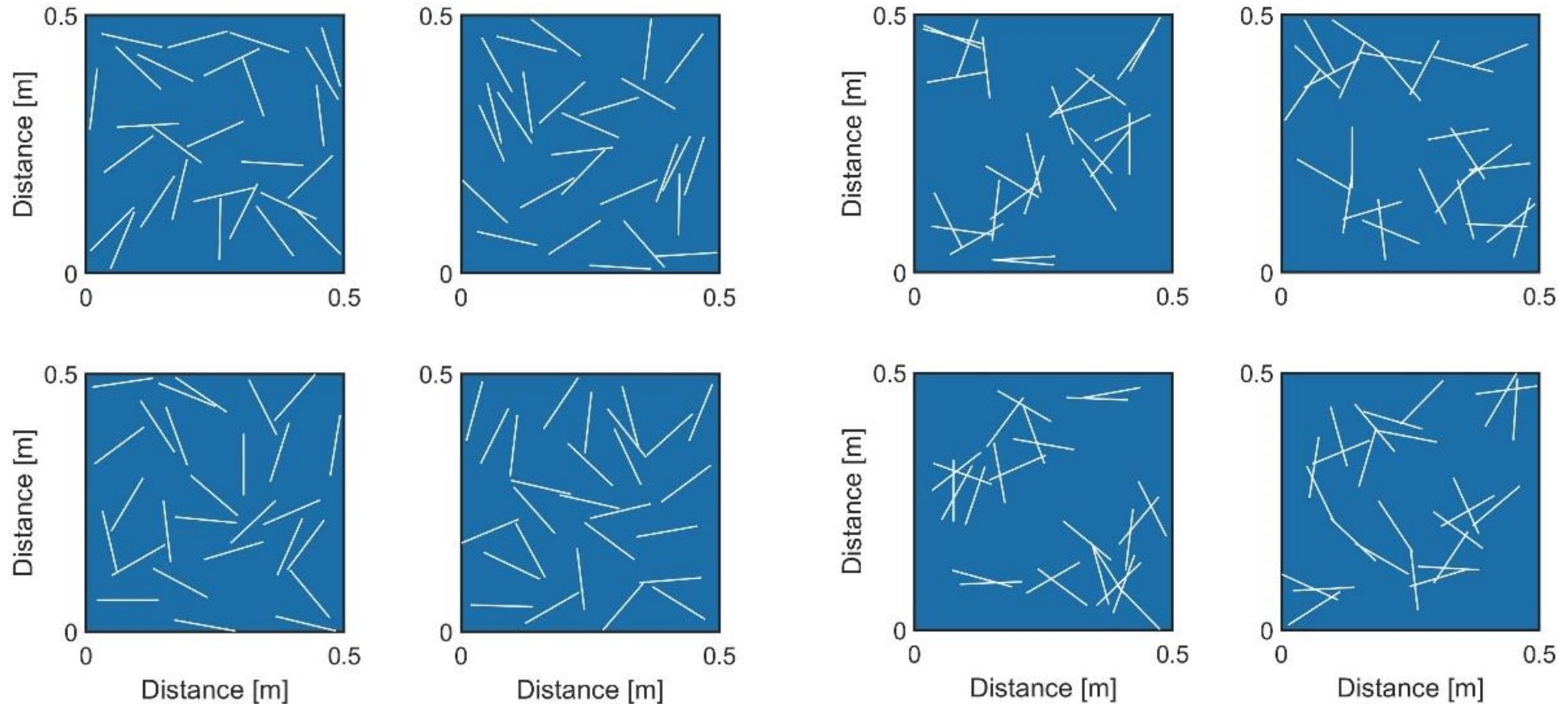
The properties of the background correspond to granite (Detournay and Cheng, 1993). The fracture and fluid properties are adapted from Rubino et. al. (2017).

Property	Background	Fracture
Solid grain density	2700 kg/m <sup>3</sup>	2700 kg/m <sup>3</sup>
Solid grain Bulk Modulus	45 GPa	45 GPa
Dry frame shear modulus	19 GPa	0.02 GPa
Dry frame bulk modulus	35 GPa	0.04 GPa
Permeability	1e-7 D	1e2 D
Porosity	0.02	0.8
Viscosity	1e-3 Pa.s	1e-3 Pa.s
Fluid bulk modulus	2.25 GPa	2.25 GPa
Fluid density	1090 kg/m <sup>3</sup>	1090 kg/m <sup>3</sup>



# Effective body wave velocities

## End-member-type scenarios of fracture network connectivity



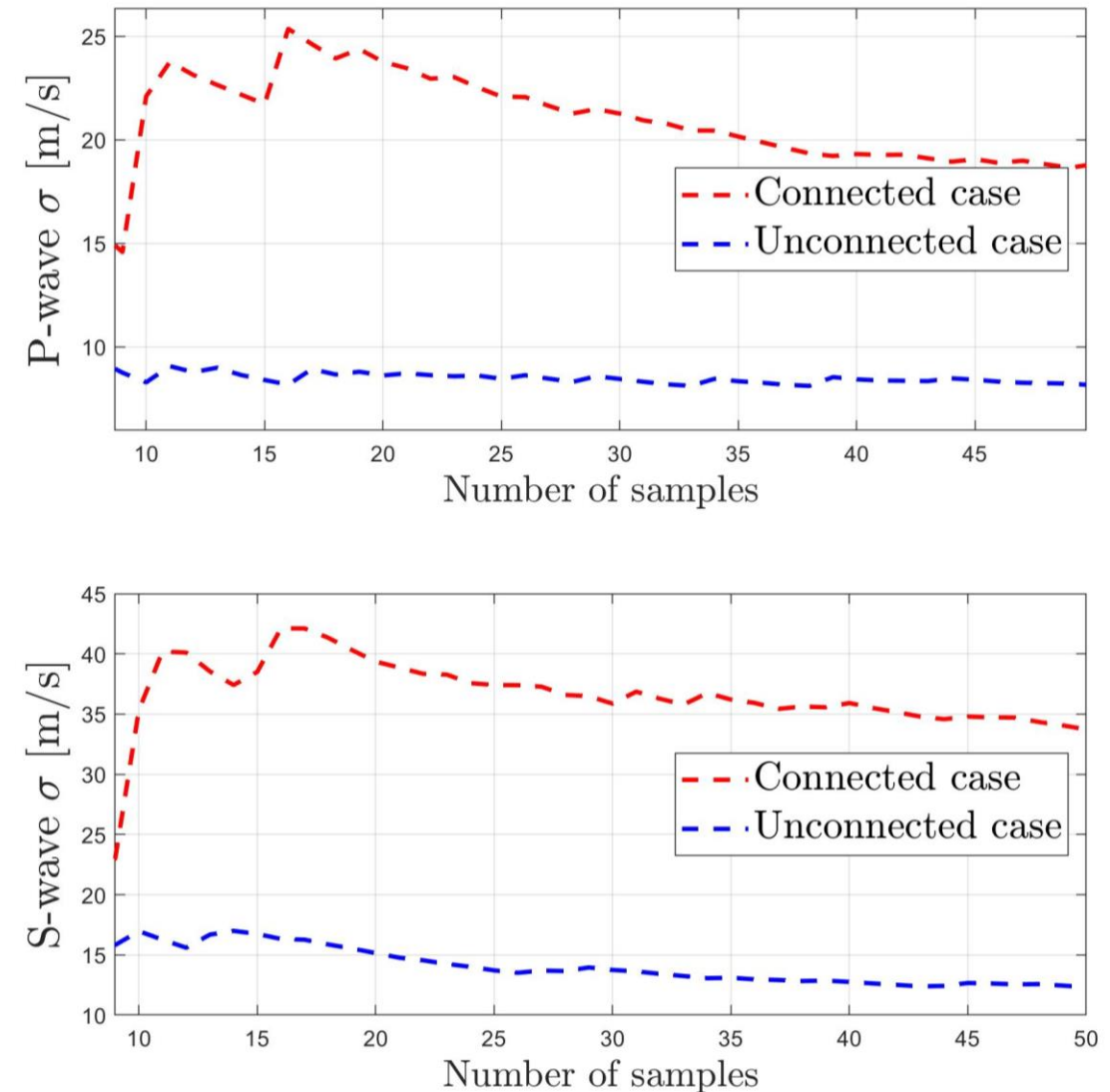
Examples of fracture networks where there is no connection between fractures

Examples of fracture networks with at least a connection per fracture

# Effective body wave velocities

We applied the poroelastic upscaling procedure on 50 samples with completely unconnected randomly distributed fractures and 50 samples where each fracture has at least a connection with another one.

The figure shows the evolution of the standard deviation,  $\sigma$ , of the P- and S-wave velocities as functions of the number of realizations for a frequency of 1 Hz. This number of samples satisfies the convergence criterion of stability of the standard deviation.

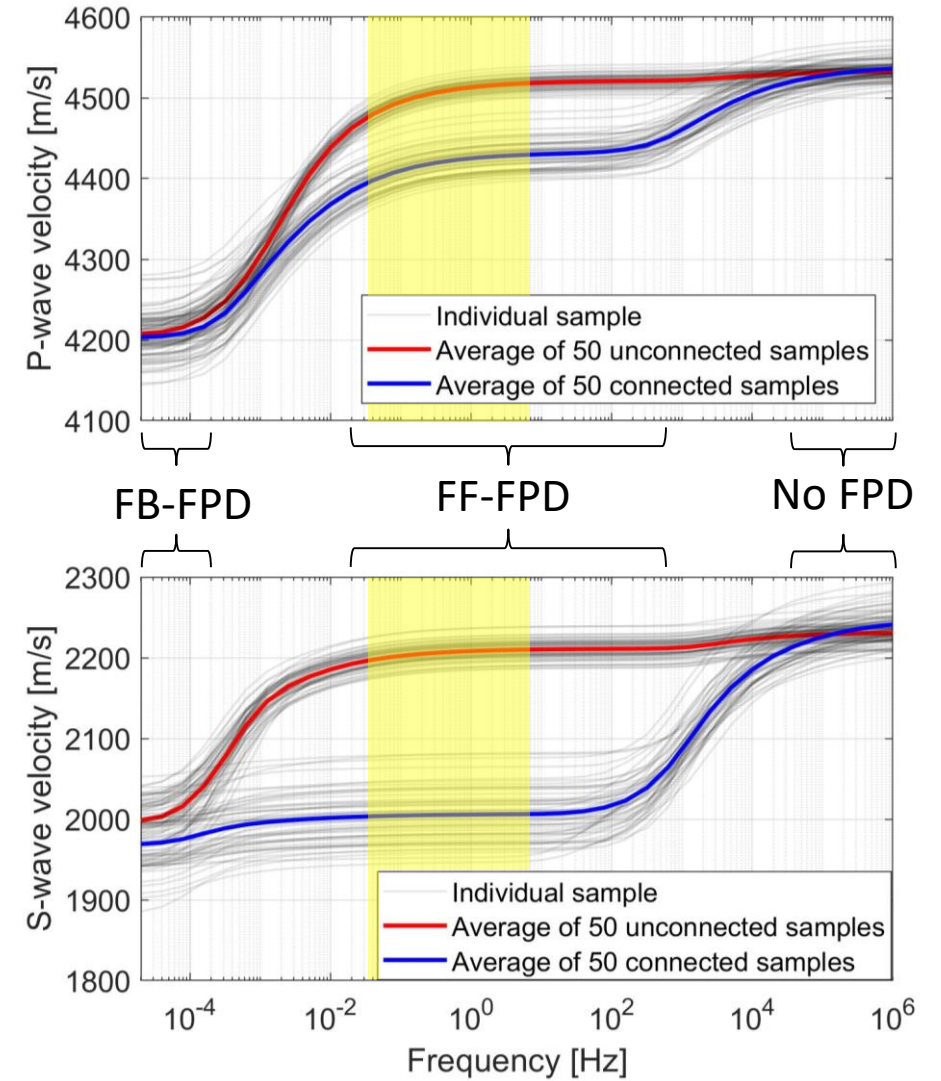


# Effective body wave velocities

The figure shows the corresponding P- and S-wave velocities as functions of frequency for each realization (grey curves) as well as the resulting averages of each 50 samples set.

There is a systematic differentiation for the connected and unconnected case particularly in the range from  $10^{-2}$  to  $10^2$  Hz, due to a reduction of the stiffening effect of the fracture pore fluid as consequence of FF-FPD (Rubino et. al. 2017).

Above  $10^5$  Hz, there is no FPD and the response of the sample is equivalent to that of a corresponding elastic composite. For this reason, the samples containing connected or unconnected fractures have a very similar mechanical response, as predicted by the analysis of Grechka and Kachanov (2006). This shows that the differentiation observed is due to FPD effects and not to geometric changes between the connected and unconnected samples.



Highlighted in yellow the frequency range employed in the Rayleigh wave analysis

# Rayleigh wave velocity dispersion analysis

The reservoir models used in the calculation of the Rayleigh wave dispersion curves are shown in the tables. For the frequencies considered, from  $5 \cdot 10^{-2}$  to 2 Hz, the velocity dispersion of the effective body wave velocities is negligible, as shown in the previous figure, and, for this reason, the use of a model of isotropic, elastic layers is valid.

We consider four 1D models of two layers over a half-space, corresponding to sandstone, a fractured granite reservoir and to non-fractured granitic rocks, as shown in the table.

The properties of the second layer correspond to the resulting values of the Monte Carlo procedure for the connected and unconnected fracture networks. We will also consider the elastic equivalent limit of the procedures considering the values of the effective velocities for a frequency of  $10^6$  Hz.

Layer thickness [m]	P-velocity [m/s]	S-velocity [m/s]	Density [kg/m <sup>3</sup> ]
Unconnected model			
2500	3500	2000	2500
700	4510	2210	2690
Infinite	4810	2620	2700
Connected model			
2500	3500	2000	2500
700	4425	2005	2690
Infinite	4810	2620	2700
Unconnected elastic model			
2500	3500	2000	2500
700	4532	2230	2690
Infinite	4810	2620	2700
Connected elastic model			
2500	3500	2000	2500
700	4536	2241	2690
Infinite	4810	2620	2700

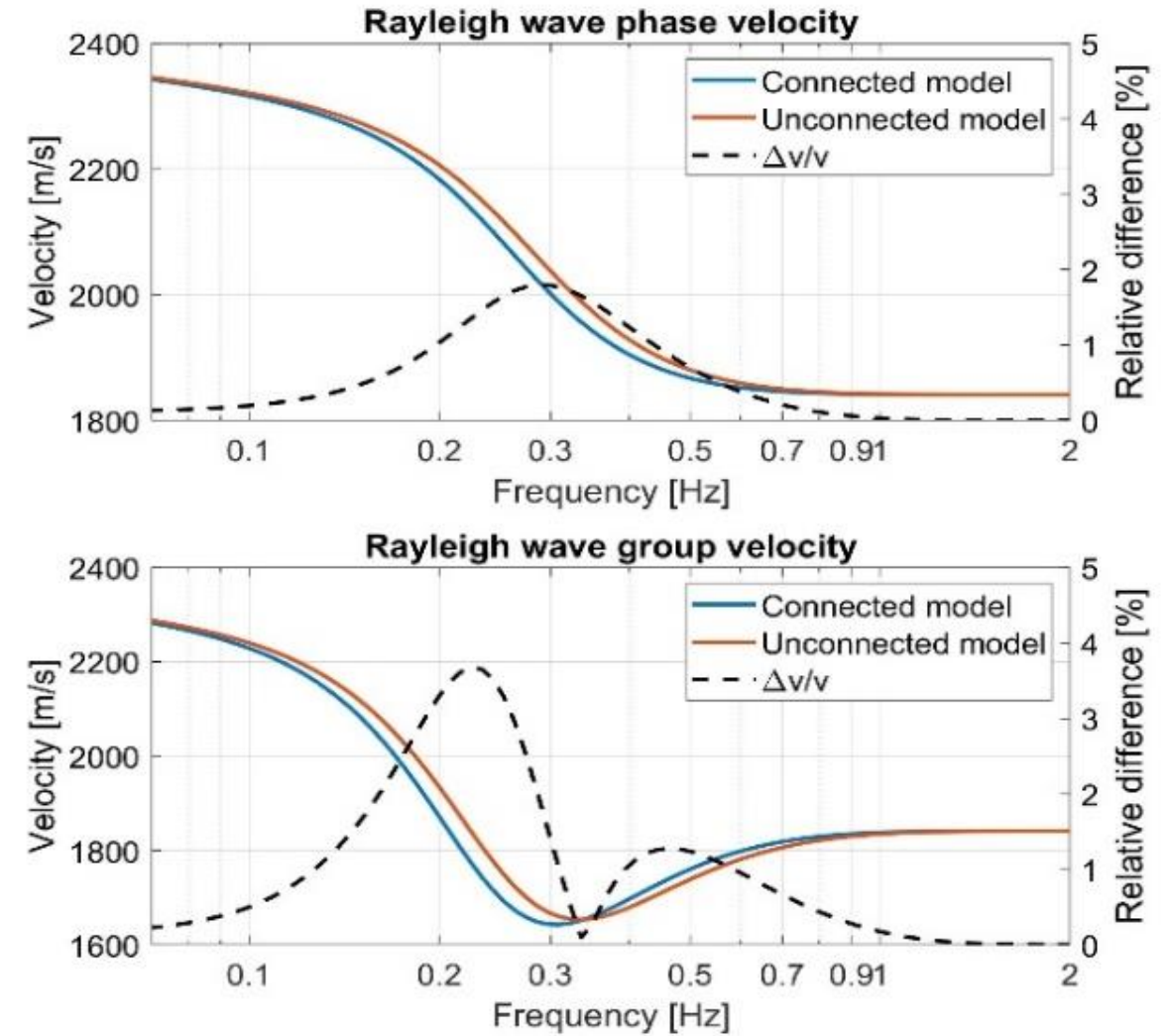


# Rayleigh wave velocity dispersion analysis

Comparison of the results obtained for the Rayleigh wave velocity dispersion for the connected and unconnected reservoir models taking into account FPD effects.

There is a relative difference of up to 4% for group velocities and 3% for phase velocities between the connectivity cases.

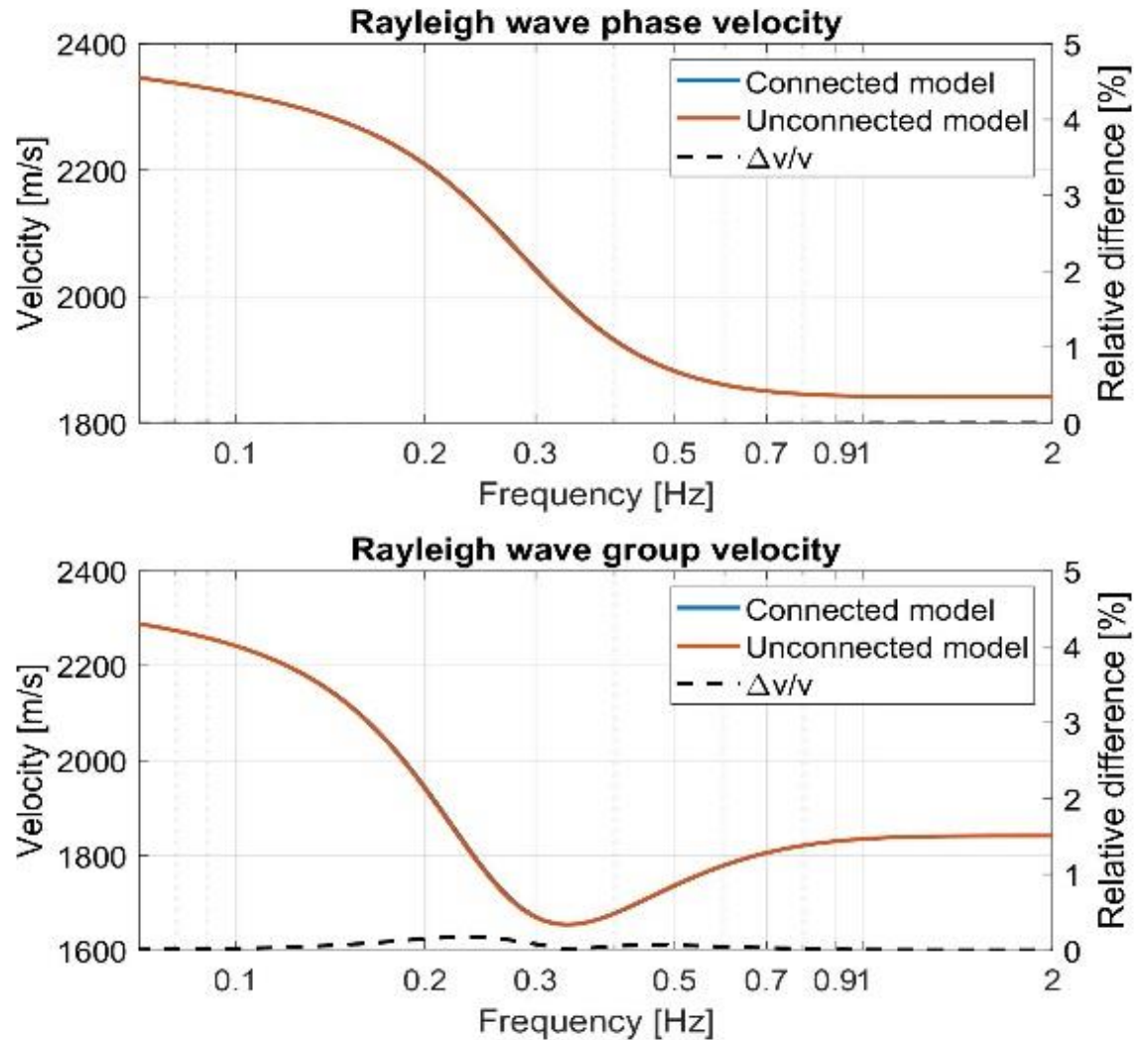
These differences are one order-of-magnitude larger than the recent results of passive monitoring of a geothermal reservoir by Taira et. al. (2018) who attributed these velocity decreases to enhanced fracture density due to an increase in seismic activity.



Relative difference  $\Delta v/v$  computed as the ratio of the difference over the average of the respective curves

# Rayleigh wave velocity dispersion analysis

Comparison of the reservoir models in an elastic scenario, considering the effective velocities for a frequency of  $10^6$  Hz shows that the differences are largely negligible. This further confirms that the differences observed in the previous figure are to be attributed to FPD effects and not to geometrical changes in the fracture networks for each case.



Relative difference  $\Delta v/v$  computed as the ratio of the difference over the average of the respective curves

# Conclusions

Our results show that FPD effects have a significant impact on Rayleigh wave velocity dispersion in fractured rocks on the frequencies in which passive seismic monitoring is usually carried on.

While velocity decreases in time-lapse monitoring are commonly attributed to increases in fracture density, this work demonstrates that changes in fracture connectivity and the FPD effects associated with them may also explain such observations.

As it is expected that the seismic activity linked to exploitation of geothermal reservoirs or similar activities does not only affect the density of fractures but also their degree of connectivity, it is important to account for the associated effects of FPD in corresponding passive seismic monitoring.



# References

Buchen, P. W., & Ben-Hador, R. (1996). Free-mode surface-wave computations. *Geophysical Journal International*, 124(3), 869-887.

Detournay, E., & Cheng, A. H. D. (1993). Fundamentals of poroelasticity. Volume II of *Comprehensive Rock Engineering: Principles, Practice & Projects.*, Chapter 5.

Favino, M., Hunziker, J., Caspari, E., Quintal, B., Holliger, K. & Krause, R. (2020). Fully-automated adaptive mesh refinement for media embedding complex heterogeneities: application to poroelastic fluid pressure diffusion. *Computational Geosciences*.  
<https://doi.org/10.1007/s10596-019-09928-2>.

Germán Rubino, J., Guarracino, L., Müller, T. M., & Holliger, K. (2013). Do seismic waves sense fracture connectivity?. *Geophysical Research Letters*, 40(4), 692-696.

Grechka, V., & Kachanov, M. (2006). Effective elasticity of rocks with closely spaced and intersecting cracks. *Geophysics*, 71(3), D85-D91.

Hunziker, J., Favino, M., Caspari, E., Quintal, B., Rubino, J. G., Krause, R., & Holliger, K. (2018). Seismic attenuation and stiffness modulus dispersion in porous rocks containing stochastic fracture networks. *Journal of Geophysical Research: Solid Earth*, 123(1), 125-143.

Obermann, A., Kraft, T., Larose, E., & Wiemer, S. (2015). Potential of ambient seismic noise techniques to monitor the St. Gallen geothermal site (Switzerland). *Journal of Geophysical Research: Solid Earth*, 120(6), 4301-4316.

Rubino, J. G., Caspari, E., Müller, T. M., Milani, M., Barbosa, N. D., & Holliger, K. (2016). Numerical upscaling in 2-D heterogeneous poroelastic rocks: Anisotropic attenuation and dispersion of seismic waves. *Journal of Geophysical Research: Solid Earth*, 121(9), 6698-6721.

Rubino, J. G., Müller, T. M., Guarracino, L., Milani, M., & Holliger, K. (2014). Seismoacoustic signatures of fracture connectivity. *Journal of Geophysical Research: Solid Earth*, 119(3), 2252-2271.

Rubino, J. G., Ravazzoli, C. L., & Santos, J. E. (2009). Equivalent viscoelastic solids for heterogeneous fluid-saturated porous rocks. *Geophysics*, 74(1), N1-N13.

Rubino, J., Caspari, E., Müller, T. M., & Holliger, K. (2017). Fracture connectivity can reduce the velocity anisotropy of seismic waves. *Geophysical Journal International*, 210(1), 223-227.

Taira, T. A., Nayak, A., Brenguier, F., & Manga, M. (2018). Monitoring reservoir response to earthquakes and fluid extraction, Salton Sea geothermal field, California. *Science Advances*, 4(1), e1701536.

# Acknowledgements

This work is supported by a grant from the Swiss National Science Foundation and has been completed within the Swiss Competence Center on Energy Research – Supply of Electricity, with the support of Innosuisse.

J. G. R. gratefully acknowledges the financial support received from the Agencia Nacional de Promoción Científica y Tecnológica of Argentina (PICT 2017-2976).